IET Control Theory & Applications

Research Article

IET Journals
The Institution of Engineering and Technology

Observer-based non-linear H_∞ attitude control for a flexible satellite

ISSN 1751-8644
Received on 7th March 2017
Revised 15th May 2017
Accepted on 31st May 2017
E-First on 4th July 2017
doi: 10.1049/iet-cta.2017.0129
www.ietdl.org

Huihui Bai[1], Yanru Zhou[1], Hongfei Sun[1], Jianping Zeng[1] ✉

[1]*Department of Automation, Xiamen University, Xiamen 361005, Fujian, People's Republic of China*

✉ *E-mail: jpzeng@xmu.edu.cn*

Abstract: This study focuses on the observer-based non-linear H_∞ (OBNH) attitude control for a flexible satellite with external disturbances and local state-region constraints. By considering the structural features of the attitude system and applying Lyapunov stability theory, the solvable conditions of the OBNH attitude control problem are provided. An advantage of this study is that the state-feedback controller and the reduced-order state observer can be designed independently, thus significantly reducing the complexity of the attitude control algorithm. Furthermore, based on the polynomial sum of squares (SOSs) and the generalised *S*-procedure techniques, the above problem can be transformed into a convex optimisation problem with SOS constraints. This conversion can effectively overcome the computational difficulties widely present in the control problem of non-linear systems. Finally, a numerical example is given to illustrate the effectiveness and feasibility of the proposed approach.

1 Introduction

The attitude control with high pointing accuracy for a flexible satellite is a challenging problem, because the control object is a complex multi-input and multi-output system involving strong non-linearity, flexible structures and unknown parameters. Owing to the lack of general non-linear design theories and methodologies, the approximate linearisation technique is still the basic way to address the spacecraft attitude control problems, which has been proven to be an effective one in space engineering [1, 2]. However, the outcome of approximate linearisation is essentially a local one which limits the applications to the large-angle attitude manoeuvring for spacecraft. To realise the increasing complex engineering task, it is necessary to carry out research on non-linear control theory. In recent years, to address the disturbances, uncertainties, saturation and the other input non-linearity of spacecraft, the intelligent-based control methods (such as adaptive-based control method [3], fuzzy-based control method [4], disturbance observer-based control method [5] and neural networks based control method [6, 7]) and the non-linear robust control methods [such as non-linear H_∞ control (NHC) method [8, 9]] are usually adopted. In this paper, we present an observer-based NHC (OBNHC) approach to address the disturbances of a flexible satellite. However, the NHC design is generally related to one or more Hamilton Jacobi Isaacs inequalities which are non-convex and very difficult to compute.

Fortunately, the recent development in polynomial sum of squares (SOSs), a convex relaxation technique for testing non-negativity of polynomial functions, offers a new effective way to cope with non-linear control problems. Within the framework of SOS, many control problems with polynomial constraints can be converted into SOS convex programming problems. This conversion may effectively overcome the computational difficulties existed in traditional non-linear control problems. Therefore, the remarkable progress of SOS has effectively promoted the research on polynomial non-linear systems [10–13].

So far, the SOS technique has been used to deal with the analysis and synthesis problems for spacecraft, and some research has been found in the literature. For example, based on SOS technique, the stabilisation and switched control were investigated for the attitude manoeuvring of the rigid spacecraft in [14, 15]. A back-stepping/linear parameter-varying mixed control scheme was presented for the rigid satellite attitude system in [16]. The non-linear robust H_∞ control problem was studied for a rigid spacecraft attitude system in [17]. The NHC for a class of axisymmetric spacecraft attitude systems was addressed in [18].

It is well known that the output feedback control approaches are generally non-convex, and thus the computational difficulties are unavoidable [11, 17, 18]. As a result, the above research mainly adopts the state-feedback control approach and is almost confined to the attitude control of a rigid spacecraft. However, for a flexible satellite, the full-state feedback is impossible, because the flexible modes cannot be measured. Besides, the flexible dynamics affects the rigid motion, the absence of the measurements of the corresponding flexible modes will render the controller task more challenging. To deal with the problem, a reduced-order state observer is constructed in this paper to estimate the flexible modes, and then the estimated information is used for the design of the controller. In [19], an observer-based control approach was proposed for attitude stabilisation. However, the attenuation level of external disturbances was not considered, which is an important performance index and needs to be addressed. Moreover, it is often too restrictive to synthesise a globally stabilising controller, in a restricted region, local controllers will often perform better than global controllers. Therefore, it will be more meaningful to synthesise a local stabilising controller in a restricted region.

Motivated by these above, in the presence of external disturbances and state-region constraints, an SOS-based NH attitude control approach is proposed for the attitude manoeuvring and vibration suppression of a flexible satellite under the framework of output feedback, i.e. only the rigid body's states are assumed to be available, and the flexible modes are estimated by a reduced-order state observer. This approach presents that the OBNHC problem considered in this paper is transformed into an SOS convex optimisation problem, and the reduced-order state observer and the state-feedback controller are designed independently, thus dramatically reducing the computational complexity and overcoming the difficulties in constructing the Lyapunov function. Furthermore, the solvable SOS conditions obtained in this paper for the OBNHC problem of a non-linear system may be directly reduced to the linear matrix inequality (LMI) constraints for that of a linear system, accordingly, the results obtained are extensions of the classical linear HC theory.

The rest of this paper is organised as follows. In Section 2, some necessary preliminaries and the problem description are introduced. In Section 3, the existence conditions of the controller for OBNHC problem are derived. In Section 4, a numerical

© The Institution of Engineering and Technology 2017

example is given to illustrate the effectiveness of the proposed approach. Finally, Section 5 draws the conclusions.

The notations used are standard in this paper. R^n is the set of n-dimensional real vectors, $R^{m\times n}$ is the set of all real $m\times n$ matrices, $R[x]^{p\times q}$ is the set of all real $p\times q$ polynomial matrices of vector $x\in R^n$, $R[x]$ is the set of all real polynomial functions of vector $x\in R^n$, Φ_{sos} is the set of all SOS polynomials, $\boldsymbol{I}$ and $\boldsymbol{0}$ are the identity matrix and zero matrix with proper dimensions, $\text{He}(A)=A^{\text{T}}+A$ and $*$ is the symmetric block of a symmetric matrix.

2 Preliminaries and problem description

2.1 Preliminaries

Definition 1 [20]: A multivariate polynomial $p(x)=p(x_1,\ldots,x_n)$ is an SOS polynomial, if there exist polynomials $f_1(x),\ldots,f_m(x)$ such that

$$p(x)=\sum_{i=1}^{m}f_i^2(x)$$

It is clear that $p(x)\in\Phi_{\text{sos}}$ implies $p(x)\geq 0$ for all $x\in R^n$, whereas the converse is generally not true. Although a polynomial being an SOS is a sufficient condition for its non-negativity, some researchers have proved that the gap between them is not significant and they are even equivalent in some cases [21].
On the basis of Positivstellensatz theory [22], the generalised S-procedure is given as follows.

Lemma 1 [22]: Given $\{g_i(x)\}_{i=1}^m\in R[x]$, if there exist polynomial functions

$$s_1(x),\ldots,s_m(x)\in\Phi_{\text{sos}}$$

satisfying

$$g_0(x)-\sum_{i=1}^{m}s_i(x)g_i(x)\in\Phi_{\text{sos}}$$

then

$$\{x\in R^n|g_1(x)\geq 0,\ldots,g_m(x)\geq 0\}\subseteq\{x\in R^n|g_0(x)\geq 0\}$$

Lemma 2 [12]: Let $F(x)\in R[x]^{n\times n}$ be a symmetric polynomial matrix of degree $2d$ in $x\in R^n$ and $Z(x)$ be a column vector whose entries are all monomials in $x\in R^n$ with degree no greater than d, and consider the following conditions:

(i) $F(x)\geq 0$, $x\in R^n$;
(ii) $v^TF(x)v\in\Phi_{sos}$, where $v\in R^n$;
(iii) There exists a positive semi-definite matrix $\boldsymbol{Q}$ satisfying $v^{\text{T}}F(x)v=(v\otimes Z(x))^{\text{T}}\boldsymbol{Q}(v\otimes Z(x))$, where $\otimes$ denotes the Kronecker product.

Then (iii) $\Leftrightarrow$ (ii) $\Rightarrow$ (i).

Lemma 3 [19]: Suppose $B_x\subset R^n$ is a bounded and closed subset, $\Phi_1(x)\in R[x]^{p\times p}$, $\Phi_2(x)\in R[x]^{q\times q}$ and $\Phi_3(x)\in R[x]^{p\times q}$ are continuous polynomial function matrices in $x\in B_x$, then $\Phi_1(x)<0$ and $\Phi_2(x)<0$ if and only if for any given continuous polynomial function matrix $\Phi_3(x)\in R[x]^{p\times q}$, there exists a corresponding scalar $\lambda>0$, such that $\begin{bmatrix}\Phi_1(x) & \Phi_3(x)\\ \Phi_3^{\text{T}}(x) & \lambda\Phi_2(x)\end{bmatrix}<0$, for $x\in B_x$.

2.2 Problem description

The flexible satellite is composed of a main rigid body and some flexible appendages, whose attitude system is described by two sets of equations: dynamic equations and kinematic equations.

The kinematics of the satellite determines the attitude of the rigid body, and can be described by the Rodrigues parameters [23]

$$\sigma=l\tan\frac{\Theta}{2}$$

Here, $\sigma=[\sigma_1\ \ \sigma_2\ \ \sigma_3]^{\text{T}}\in R^3$ is a vector of the Rodrigues parameters, $\Theta\in R$ is the Euler rotation angle, $l\in R^3$ is the Euler principle axis. Then the kinematic equations in terms of the Rodrigues parameters can be given by

$$\dot{\sigma}=\alpha(\sigma)\omega \tag{1}$$

$$\alpha(\sigma)=\frac{1}{2}\begin{bmatrix}1+\sigma_1^2 & \sigma_1\sigma_2-\sigma_3 & \sigma_2+\sigma_1\sigma_3\\ \sigma_3+\sigma_1\sigma_2 & 1+\sigma_2^2 & \sigma_2\sigma_3-\sigma_1\\ \sigma_1\sigma_3-\sigma_2 & \sigma_2\sigma_3+\sigma_1 & 1+\sigma_3^2\end{bmatrix}$$

where $\omega=[\omega_1\ \ \omega_2\ \ \omega_3]^{\text{T}}$ denotes the angular velocity of the undeformed satellite in the body-fixed frame.

The dynamic equations describe the motion of the satellite with flexible appendages as follows [24]:

$$\begin{aligned}&I_{\text{s}}\dot{\omega}+S(\omega)I_{\text{s}}\omega+F_{\text{s}}\ddot{\eta}=T_{\text{c}}+T_{\text{d}}\\ &\ddot{\eta}+2\xi\Omega\dot{\eta}+\Omega^2\eta+F_{\text{s}}^{\text{T}}\dot{\omega}=0\end{aligned} \tag{2}$$

where $\eta=[\eta_1\ \ \cdots\ \ \eta_N]^{\text{T}}$ denotes the N-dimensional flexible modal coordinates; T_{c} is the control torque; T_{d} is the external disturbance torque; ξ and Ω denote the damping matrix and the natural frequency matrix, respectively; F_{s} is the coupling matrix between the flexible structures and the rigid body; I_{s} is the inertia matrix; and $S(\omega)=\begin{bmatrix}0 & -\omega_3 & \omega_2\\ \omega_3 & 0 & -\omega_1\\ -\omega_2 & \omega_1 & 0\end{bmatrix}$ is a skew matrix with respect to ω.

Let $\varphi=\dot{\eta}+F_{\text{s}}^{\text{T}}\omega$, $x_b=\begin{bmatrix}x_1\\x_2\end{bmatrix}=\begin{bmatrix}\sigma\\\omega\end{bmatrix}$, $x_f=\begin{bmatrix}x_3\\x_4\end{bmatrix}=\begin{bmatrix}\eta\\\varphi\end{bmatrix}$, and $n=6+2N$. Combining (1) with (2) produces the state equation of the flexible satellite attitude system as

$$\dot{x}=A(x_b)x+B_1w+B_2u \tag{3}$$

$$A(x_b)=\begin{bmatrix}A_{11}(x_b) & A_{12}\\ A_{21} & A_{22}\end{bmatrix},\ A_{12}=\begin{bmatrix}\boldsymbol{0} & \boldsymbol{0}\\ R_{\text{s}}F_{\text{s}}\Omega^2 & 2R_{\text{s}}F_{\text{s}}\xi\Omega\end{bmatrix},$$

$$A_{21}=\begin{bmatrix}\boldsymbol{0} & -F_{\text{s}}^{\text{T}}\\ \boldsymbol{0} & 2\xi\Omega F_{\text{s}}^{\text{T}}\end{bmatrix},\ A_{22}=\begin{bmatrix}\boldsymbol{0} & \boldsymbol{I}\\ -\Omega^2 & -2\xi\Omega\end{bmatrix},$$

$$A_{11}(x_b)=\begin{bmatrix}\boldsymbol{0} & \alpha(x_1)\\ \boldsymbol{0} & R_{\text{s}}\left(-S(x_2)I_{\text{s}}-2F_{\text{s}}\xi\Omega F_{\text{s}}^{\text{T}}\right)\end{bmatrix},$$

$$B_1=B_2=\begin{bmatrix}R\\ \boldsymbol{0}\end{bmatrix},\ R=\begin{bmatrix}\boldsymbol{0}\\ R_{\text{s}}\end{bmatrix},\ R_{\text{s}}=\left(I_{\text{s}}-F_{\text{s}}F_{\text{s}}^{\text{T}}\right)^{-1}$$

where $x=\left[x_b^{\text{T}}\ \ x_f^{\text{T}}\right]^{\text{T}}\in R^n$ is the state, $u=T_{\text{c}}\in R^3$ is the control input, and $w=T_{\text{d}}\in R^3$ is the external disturbance.

Suppose that the Euler rotation angle and angular velocity can be available [8, 19, 25–27], then the measured output can be defined as

$$y=x_b=C_1x,\ C_1=[\boldsymbol{I}\ \ \boldsymbol{0}] \tag{4}$$

The controlled output is chosen as

$$z=x \tag{5}$$

© The Institution of Engineering and Technology 2017

17518652, 2017, 15, Downloaded from https://ietresearch.onlinelibrary.wiley.com/doi/10.1049/iet-cta.2017.0129 by Turkey Cochrane Evidence Aid, Wiley Online Library on [13/09/2023]. See the Terms and Conditions (https://onlinelibrary.wiley.com/terms-and-conditions) on Wiley Online Library for rules of use; OA articles are governed by the applicable Creative Commons License

The control objective of this paper is to realise the fast large-angle attitude manoeuvring of the flexible satellite, and to suppress the external disturbances and the flexible vibrations to a certain degree. Since the states η and φ (which are related to the flexible modes and their derivatives) cannot be measured directly, a reduced-order state observer is adopted herein to estimate the flexible modes. Then, the problem considered in this paper is specifically described as follows.

Problem 1 (OBNHC): For the system given by (3)–(5), our objective is to design an observer-based state-feedback controller such that the corresponding closed-loop system satisfies the following conditions in a bounded and closed state region $B_x \subset R^n$:

(i) Internally stable, i.e. asymptotically stable at zero equilibrium with $w = 0$.
(ii) The L_2-gain from the disturbance input $w \in L_2[0, \infty)$ to the controlled output z is not more than the given positive scalar γ, i.e. $\int_0^\infty \| z(t) \|^2 \mathrm{d}t \le \gamma^2 \int_0^\infty \| w(t) \|^2 \mathrm{d}t$ with initial condition $x(0) = 0$, where $\| \cdot \|$ is the Euclidean norm.

3 Observer-BNHC

For the system in (3)–(5), the following reduced-order state observer is constructed to estimate the flexible modes:

$$\begin{aligned}\dot{z}_0 &= ((A_{22} - L(x_1)A_{12})L(x_1) + (A_{21} - L(x_1)A_{11}(y)))y \\ &\quad -\left(\sum_{i=1}^{3} \frac{\partial L(x_1)}{\partial \sigma_i}(\alpha_i(x_1)x_2)\right)y - L(x_1)B_{21}u \\ &\quad +(A_{22} - L(x_1)A_{12})z_0 \\ \hat{x}_f &= z_0 + L(x_1)y\end{aligned} \tag{6}$$

where z_0 is the observer state, $L(x_1)$ is the observer gain matrix, $\hat{x}_f$ is the estimate of x_f and $\alpha_i(x_1)$ is the ith row of $\alpha(x_1)$.

Remark 1: If $A(x_b)$ in (3) and $L(x_1)$ in (6) reduce to constant matrices, the system in (3)–(5) reduces to a linear system, and the state observer in (6) reduces to a Luenberger observer for a linear system [28]. Different from the traditional Luenberger observer, the observer gain matrix $L(x_1)$ is related to the sub-state x_1. Therefore, the state observer in (6) can be treated as an extension of the traditional Luenberger observer in a linear system to a non-linear polynomial system. Moreover, the rigid dynamics is influenced by the flexible appendages dynamics through the coupling matrix F_s, hence it is possible to estimate the flexible modes from the measurement information by using the state observer of the form in (6).

On the basis of the observer in (6), the state-feedback controller is selected to be of the following form:

$$u = K(x_b)\hat{x} = K(x_b)(x - We) \tag{7}$$

where $\hat{x} = \begin{bmatrix} x_b \\ \hat{x}_f \end{bmatrix}$, $e = x_f - \hat{x}_f$, $W = [\mathbf{0} \quad \boldsymbol{I}]^{\mathrm{T}}$ and $K(x_b)$ is the controller gain matrix to be designed later.

Combining (3)–(5) with (6) and (7), the corresponding closed-loop system is rewritten as

$$\begin{aligned}\dot{\zeta} &= A_\zeta(x_b)\zeta + B_\zeta w \\ z &= C_\zeta \zeta\end{aligned} \tag{8}$$

where $\zeta = \begin{bmatrix} x \\ e \end{bmatrix}$, $B_\zeta = \begin{bmatrix} B_1 \\ \mathbf{0} \end{bmatrix}$, $C_\zeta = [\boldsymbol{I} \quad \mathbf{0}]$, $A_\zeta(x_b) = \begin{bmatrix} A(x_b) + B_2K(x_b) & -B_2K(x_b)W \\ \mathbf{0} & A_{22} - L(x_1)A_{12} \end{bmatrix}$.

Then, the OBNHC problem is concerned with designing the observer of the form in (6) and the controller of the form in (7) such that the closed-loop system formulated in (8) satisfies the conditions (i)–(ii) in Problem 1.

On the basis of Lyapunov stability theory, a solvable criterion for Problem 1 is established as follows.

Lemma 4: Consider the system in (3)–(5). For a given scalar $\gamma > 0$, if there exists a positive-definite polynomial matrix $P(x_1) \in R[x]^{(n+2N)\times(n+2N)}$, two polynomial matrices $L(x_1) \in R[x]^{2N\times 6}$ and $K(x_b) \in R[x]^{3\times n}$, such that the closed-loop system formulated in (8) satisfies the following inequality:

$$\begin{aligned}\Sigma_0(x_b) &= \begin{bmatrix} \Sigma_{00}(x_b) & * & * \\ C_\zeta & -\boldsymbol{I} & * \\ B_\zeta^T P(x_1) & \mathbf{0} & -\gamma^2\boldsymbol{I} \end{bmatrix} < 0 \\ \Sigma_{00}(x_b) &= \mathrm{He}\left(P(x_1)A_\zeta(x_b) + \sum_{i=1}^{3} \frac{\partial P(x_1)}{\partial \sigma_i}(\alpha_i(x_1)x_2)\right)\end{aligned} \tag{9}$$

Then Problem 1 is solvable with the state observer of the form in (6) and the controller of form in (7).

Proof: Choose Lyapunov function for the closed-loop system formulated in (8) as

$$V(\zeta) = \zeta^{\mathrm{T}} P(x_1)\zeta$$

When $w = 0$, from the condition in (9), we have

$$\begin{aligned}\dot{V}(\zeta) &= \zeta^{\mathrm{T}}\Pi(x_b)\zeta < 0 \\ \Pi(x_b) &= \mathrm{He}\big(P(x_1)A_\zeta(x_b)\big) + \sum_{i=1}^{3} \frac{\partial P(x_1)}{\partial \sigma_i}(\alpha_i(x_1)x_2)\end{aligned}$$

which implies that the closed-loop system in (8) is internally stable. When $x(0) = 0$, $w \in L_2[0, \infty)$, for any $T_0 > 0$, define

$$J = \int_0^{\mathrm{T}_0} \left(z^{\mathrm{T}}z - \gamma^2 w^{\mathrm{T}}w\right)\mathrm{d}t$$

then

$$\begin{aligned}J &= \int_0^{T_0} \left(z^{\mathrm{T}}z - \gamma^2 w^{\mathrm{T}}w + \dot{V}(\zeta)\right)\mathrm{d}t - V(\zeta(T_0)) \\ &\le \int_0^{T_0} \left(z^{\mathrm{T}}z - \gamma^2 w^{\mathrm{T}}w + \dot{V}(\zeta)\right)\mathrm{d}t \\ &\le \int_0^{T_0} \left(\varsigma^{\mathrm{T}}\Phi_0(x_b)\varsigma\right)\mathrm{d}t\end{aligned}$$

where $\varsigma = \begin{bmatrix} \zeta \\ w \end{bmatrix}$, $\Phi_0(x_b) = \begin{bmatrix} \Sigma_{00}(x_b) + C_\zeta^{\mathrm{T}}C_\zeta & * \\ B_\zeta^{\mathrm{T}}P(x_1) & -\gamma^2\boldsymbol{I} \end{bmatrix}$.
Let $T_0 \to \infty$, by the condition in (9) and Schur complement lemma, we have

$$\int_0^\infty \left(z^{\mathrm{T}}z - \gamma^2 w^{\mathrm{T}}w\right)\mathrm{d}t \le 0$$

which implies that the L_2-gain of the closed-loop system in (8) is not more than γ. □

In Lemma 4, the condition in (9) is difficult to solve, because the interference of the cross-couplings generated by the polynomial matrix variables $P(x_1)$, $K(x_b)$ and $L(x_1)$ makes it non-convex. Fortunately, when the states are restricted to a bounded and closed region, by Lemma 3, we may convert the non-convex condition in (9) into some equivalent state-dependent LMI constraints formulated in the following lemma. Accordingly, the state observer gain matrix in (6) and the controller gain matrix in (7) can be

© The Institution of Engineering and Technology 2017

17518652, 2017, 15, Downloaded from https://ietresearch.onlinelibrary.wiley.com/doi/10.1049/iet-cta.2017.0129 by Turkey Cochrane Evidence Aid, Wiley Online Library on [13/09/2023]. See the Terms and Conditions (https://onlinelibrary.wiley.com/terms-and-conditions) on Wiley Online Library for rules of use; OA articles are governed by the applicable Creative Commons License

analytically constructed. Furthermore, in condition (9), $\Sigma_0(x_b)$ is only the polynomial matrix of the sub-states x_b, hence the bounded and closed state region can be only restricted for x_b according to Lemma 3 and denoted by B_{x_b} herein.

Lemma 5: Suppose x_b belongs to a bounded and closed subset B_{x_b} in the system given by (3)–(5). For a given scalar $\gamma > 0$, there exist positive-definite polynomial matrices $P_1(x_1) \in R[x]^{n\times n}$ and $P_2(x_1) \in R[x]^{2N\times 2N}$, such that the following statements are equivalent in $x_b \in B_{x_b}$:

(i) There exist two polynomial matrices $K(x_b) \in R[x]^{3\times n}$ and $L(x_1) \in R[x]^{2N\times 6}$, a constant $\lambda > 0$, and a positive-definite matrix $P(x_1) = \text{diag}\{P_1^{-1}(x_1),\ \lambda P_2(x_1)\}$, such that the condition in (9) holds.

(ii) There exist two polynomial matrices $X(x_b) \in R[x]^{3\times n}$ and $Y(x_1) \in R[x]^{2N\times 6}$, such that

$$\Sigma_1(x_b) = \begin{bmatrix} \Sigma_{11}(x_b) & * & * \\ P_1(x_1) & -\boldsymbol{I} & * \\ B_1^T & \boldsymbol{0} & -\gamma^2\boldsymbol{I} \end{bmatrix} < 0 \tag{10}$$

$$\Sigma_2(x_1) = \text{He}(P_2(x_1)A_{22} - Y(x_1)A_{12}) + \sum_{i=1}^{3} \frac{\partial P_2(x_1)}{\partial \sigma_i}(\alpha_i(x_1)x_2) < 0 \tag{11}$$

$$\Sigma_{11}(x_b) = \text{He}(A(x_b)P_1(x_1) + B_2X(x_b)) - \sum_{i=1}^{3} \frac{\partial P_1(x_1)}{\partial \sigma_i}(\alpha_i(x_1)x_2)$$

Furthermore, if the statement in (ii) is satisfied, Problem 1 is solvable with the corresponding state observer gain matrix in (6) and controller gain matrix in (7) being, respectively, given by

$$L(x_1) = P_2^{-1}(x_1)Y(x_1) \tag{12}$$

and

$$K(x_b) = X(x_b)P_1^{-1}(x_1) \tag{13}$$

Proof: (i) ⇒ (ii)
From the condition in (9) and $P(x_1) = \text{diag}\{P_1^{-1}(x_1),\ \lambda P_2(x_1)\}$, we obtain

$$\Sigma_0(x_b) = \begin{bmatrix} \Sigma_{011}(x_b) & * & * & * \\ \Sigma_{021}(x_b) & \Sigma_{022}(x_1) & * & * \\ \boldsymbol{I} & \boldsymbol{0} & -\boldsymbol{I} & * \\ B_1^{\text{T}}P_1^{-1}(x_1) & \boldsymbol{0} & \boldsymbol{0} & -\gamma^2\boldsymbol{I} \end{bmatrix} < 0 \tag{14}$$

$$\Sigma_{011}(x_b) = \text{He}\big(P_1^{-1}(x_1)(A(x_b) + B_2K(x_b))\big) + \sum_{i=1}^{3} \frac{\partial P_1^{-1}(x_1)}{\partial \sigma_i}(\alpha_i(x_1)x_2)$$

$$\Sigma_{021}(x_b) = -(B_2K(x_b)W)^{\text{T}}P_1^{-1}(x_1)$$

$$\Sigma_{022}(x_1) = \text{He}(P_2(x_1)(A_{22} - L(x_1)A_{12})) + \sum_{i=1}^{3} \frac{\partial P_2(x_1)}{\partial \sigma_i}(\alpha_i(x_1)x_2)$$

Multiplying both sides of the inequality in (14) by $\text{diag}\{P_1(x_1), \boldsymbol{0}, \boldsymbol{I}, \boldsymbol{I}\}$ and denoting $K(x_b)P_1(x_1) = X(x_b)$, then the condition in (10) holds by Schur complement lemma.
Similarly, multiplying both sides of the inequality in (14) by $\text{diag}\{\boldsymbol{0}, \boldsymbol{I}, \boldsymbol{0}, \boldsymbol{0}\}$ and denoting $P_2(x_1)L_1(x_1) = Y(x_1)$, then the condition in (11) holds

(ii) ⇒ (i)

Let $L(x_1) = P_2^{-1}(x_1)Y(x_1)$, $K(x_b) = X(x_b)P_1^{-1}(x_1)$, the conditions in (10) and (11) can be, respectively, rewritten as

$$\hat{\Sigma}_1(x_b) = \begin{bmatrix} \Sigma_{011}(x_b) & * & * \\ \boldsymbol{I} & -\boldsymbol{I} & * \\ B_1^{\text{T}}P_1^{-1}(x_1) & \boldsymbol{0} & -\gamma^2\boldsymbol{I} \end{bmatrix} < 0$$

and

$$\hat{\Sigma}_2(x_1) = \Sigma_{022}(x_1) < 0$$

Let $\Sigma_3(x_b) = \begin{bmatrix}\Sigma_{021}(x_b) & \boldsymbol{0} & \boldsymbol{0}\end{bmatrix}^{\text{T}}$, according to Lemma 3, there exists a corresponding scalar $\lambda > 0$ satisfying

$$\begin{bmatrix} \hat{\Sigma}_1(x_b) & \Sigma_3(x_b) \\ \Sigma_3^{\text{T}}(x_b) & \lambda\hat{\Sigma}_2(x_1) \end{bmatrix} < 0 \tag{15}$$

which implies that the condition in (9) holds by denoting $P(x_1) = \text{diag}\{P_1^{-1}(x_1), \lambda P_2(x_1)\}$. □

Remark 2: In Lemma 5, the inequalities in (10) and (11) are the existence conditions of the controller in (7) and the observer in (6), respectively, and there is no coupling of the variables between them. It indicates that the state-feedback controller and the reduced-order observer can be designed independently. This property is similar to a separation principle in a linear system which is difficult to satisfy in a non-linear system. Hence, such results are very rare in non-linear systems, except the reference in [29], in which the matrix decoupling technique was presented for the Takagi–Sugeno fuzzy systems with state delays.

Although the conditions (10) and (11) in Lemma 5 are state-dependent LMIs, which hold for any bounded and closed state region B_{x_b}, when the forms of B_{x_b} is not formulated specifically, the solutions of Problem 1 are still difficult to calculate. Since the state-region constraints should be added into the conditions (10) and (11) to search for a local solution, if the form of B_{x_b} is implicit, it may be very difficult to handle.

Therefore, in order to obtain the computationally tractable conditions, the bounded and closed state-region B_{x_b} should be given in an explicit form. For the sake of simplicity, we only choose the following form of state region as an example:

$$B_{x_b} = \left\{ x_b = \begin{bmatrix}\sigma \\ \omega\end{bmatrix} \in R^6 : R_i = \delta_i^2 - \sigma_i^2 \geq 0,\ R_{3+i} = \pi_i^2 - \omega_i^2 \geq 0,\ i = 1,\ 2,\ 3 \right\} \tag{16}$$

where δ_i and π_i ($i = 1, 2, 3$) are any given positive constants.

Remark 3: In B_{x_b}, δ_i and π_i ($i = 1, 2, 3$) are properly given according to the engineering practise. For instance, to ensure the control objective of the principal angle Θ to be within $[-90^\circ\ \ 90^\circ]$, one has $|\sigma_1| \leq 1$, hence δ_1 must be no less than 1.
In such situation, based on the SOS technique and the generalised *S*-procedure, the state-dependent LMI conditions in (10) and (11) with the state-region constraint in (16) is transformed into the corresponding SOS constraints formulated in the following theorem and can be directly solved by MATLAB toolbox SOSTOOLS [20].

Theorem 1: Consider the system in (3)–(5). For a given scalar $\gamma > 0$, polynomial functions $\varepsilon_1(x_1) > 0$, $\varepsilon_2(x_b) > 0$, $\varepsilon_3(x_1) > 0$, $\varepsilon_4(x_1) > 0$, if there exist the positive-definite polynomial matrices $P_1(x_1) \in R[x]^{n\times n}$, $P_2(x_1) \in R[x]^{2N\times 2N}$, the polynomial matrices $X(x_b) \in R[x]^{3\times n}$, $Y(x_1) \in R[x]^{2N\times 6}$ and the SOS polynomial

© The Institution of Engineering and Technology 2017

17518652, 2017, 15, Downloaded from https://ietresearch.onlinelibrary.wiley.com/doi/10.1049/iet-cta.2017.0129 by Turkey Cochrane Evidence Aid, Wiley Online Library on [13/09/2023]. See the Terms and Conditions (https://onlinelibrary.wiley.com/terms-and-conditions) on Wiley Online Library for rules of use; OA articles are governed by the applicable Creative Commons License

functions $\kappa_{1i}(x_1)$, $\tau_{1j}(x_b)$, $\kappa_{2i}(x_1)$, $\tau_{1i}(x_1)$ ($i = 1, 2, 3$, $j = 1, 2, \ldots, 6$), such that

$$v_1^{\mathrm{T}}(P_1(x_1) - \varepsilon_1(x_1)\boldsymbol{I})v_1 - \upsilon_1^{\mathrm{T}}\Lambda_1\upsilon_1 \in \Phi_{\mathrm{sos}} \tag{17}$$

$$-v_2^{\mathrm{T}}(\Sigma_1(x_b) + \varepsilon_2(x_b)\boldsymbol{I})v_2 - \upsilon_2^{\mathrm{T}}\Lambda_2\upsilon_2 \in \Phi_{\mathrm{sos}} \tag{18}$$

$$v_3^{\mathrm{T}}(P_2(x_1) - \varepsilon_3(x_1)\boldsymbol{I})v_3 - \upsilon_3^{\mathrm{T}}\Lambda_3\upsilon_3 \in \Phi_{\mathrm{sos}} \tag{19}$$

$$-v_4^{\mathrm{T}}(\Sigma_2(x_1) + \varepsilon_4(x_1)\boldsymbol{I})v_4 - \upsilon_4^{\mathrm{T}}\Lambda_4\upsilon_4 \in \Phi_{\mathrm{sos}} \tag{20}$$

$$\begin{aligned}
\Lambda_1 &= \mathrm{diag}\{\kappa_{11}(x_1)R_1,\ \kappa_{12}(x_1)R_2,\ \kappa_{13}(x_1)R_3\}\\
\Lambda_2 &= \mathrm{diag}\{\tau_{11}(x_b)R_1,\ \tau_{12}(x_b)R_2,\ \tau_{13}(x_b)R_3,\\
&\qquad \tau_{14}(x_b)R_4,\ \tau_{15}(x_b)R_5,\ \tau_{16}(x_b)R_6\}\\
\Lambda_3 &= \mathrm{diag}\{\kappa_{21}(x_1)R_1,\ \kappa_{22}(x_1)R_2,\ \kappa_{23}(x_1)R_3\}\\
\Lambda_4 &= \mathrm{diag}\{\tau_{21}(x_1)R_1,\ \tau_{22}(x_1)R_2,\ \tau_{23}(x_1)R_3\}
\end{aligned}$$

where $v_1 \in R^n$, $v_2 \in R^{n+9}$, $v_3 \in R^{2N}$ and $v_4 \in R^{2N}$; υ_2 is a vector consisting of any six elements of v_2; υ_1, υ_3 and υ_4 are vectors consisting of any three elements of v_1, v_3 and v_4, respectively. Then, Problem 1 is solvable with the corresponding state observer gain matrix in (6) and controller gain matrix in (7) being given by (12) and (13), respectively. Furthermore, the sub-states x_b of the system satisfy the constraint given by (16).

Proof: Denote

$$\Xi(v_1, \upsilon_1, x_1) = v_1^{\mathrm{T}}(P_1(x_1) - \varepsilon_1(x_1)\boldsymbol{I})v_1 - \upsilon_1^{\mathrm{T}}\Lambda_1\upsilon_1$$

and

$$\begin{aligned}
s_i(v_1, \upsilon_1, x_1) &= \upsilon_{1i}^{\mathrm{T}}\kappa_{1i}(x_1)\upsilon_{1i} = \upsilon_{1i}^2\kappa_{1i}(x_1) \geq 0\\
\upsilon_1 &= \begin{bmatrix}\upsilon_{11} & \upsilon_{12} & \upsilon_{13}\end{bmatrix}^{\mathrm{T}}
\end{aligned}$$

From the condition in (17), we have

$$\begin{aligned}
\Xi(v_1, \upsilon_1, x_1) &= v_1^{\mathrm{T}}(P_1(x_1) - \varepsilon_1(x_1)\boldsymbol{I})v_1 - \sum_{i=1}^{3}\upsilon_{1i}^{\mathrm{T}}\kappa_{1i}(x_1)R_i(x_b)\upsilon_{1i}\\
&= v_1^{\mathrm{T}}(P_1(x_1) - \varepsilon_1(x_1)\boldsymbol{I})v_1 - \sum_{i=1}^{3}s_i(v_1, \upsilon_1, x_1)R_i(x_b)\\
&\geq 0
\end{aligned} \tag{21}$$

Since $R_i \geq 0$ ($i = 1, 2, 3$) in the state-region constraint given by (16), the inequality in (21) implies $P_1(x_1) > 0$ by Lemmas 1 and 2. Similarly, the conditions in (18), (19) and (20) imply $P_2(x_1) > 0$, $\Sigma_1(x_b) < 0$ and $\Sigma_2(x_1) < 0$, respectively.

Finally, by Lemmas 4 and 5, Problem 1 is solvable with the corresponding controller and observer gain matrices being given by (12) and (13), respectively. □

To reduce the design complexity and computational burden, the following corollary is obtained by restricting the polynomial matrices $P_1(x_1)$ and $P_2(x_1)$ in Theorem 1 to be constant matrices.

Corollary 1: Consider the system in (3)–(5). For the given scalars $\gamma > 0$ and $\varepsilon_i > 0$ ($i = 1, 2, 3, 4$), if there exist positive-definite constant matrices $P_1 \in R^{n\times n}$, $P_2 \in R^{2N\times 2N}$, Polynomial matrices $X(x_b) \in R[x]^{3\times n}$, $Y(x_1) \in R[x]^{2N\times 6}$ and constants $\mu_{1i} \geq 0$, $\mu_{2j} \geq 0$ ($i = 1, 2, \ldots, 6$, $j = 1, 2, 3$), such that

$$v_1^{\mathrm{T}}(P_1 - \varepsilon_1\boldsymbol{I})v_1 \in \Phi_{\mathrm{sos}} \tag{22}$$

$$-v_2^{\mathrm{T}}(\Xi_1(x_b) + \varepsilon_2\boldsymbol{I})v_2 - \sum_{i=1}^{6}\mu_{1i}R_i\upsilon_{2i}^2 \in \Phi_{\mathrm{sos}} \tag{23}$$

$$v_3^{\mathrm{T}}(P_2 - \varepsilon_3\boldsymbol{I})v_3 \in \Phi_{\mathrm{sos}} \tag{24}$$

$$-v_4^{\mathrm{T}}(\Xi_2(x_1) + \varepsilon_4\boldsymbol{I})v_4 - \sum_{j=1}^{3}\mu_{2j}R_j\upsilon_{4j}^2 \in \Phi_{\mathrm{sos}} \tag{25}$$

where

$$\begin{aligned}
\Xi_1(x_b) &= \begin{bmatrix}\mathrm{He}(A(x_b)P_1 + B_2X(x_b)) & * & *\\ P_1 & -\boldsymbol{I} & *\\ B_1^T & \boldsymbol{0} & -\gamma^2\boldsymbol{I}\end{bmatrix}\\
\Xi_2(x_1) &= \mathrm{He}(P_2A_{22} - Y(x_1)A_{12})
\end{aligned}$$

Then, Problem 1 is solvable, and in this case, the corresponding state observer gain matrix and controller gain matrix are given by $L(x_1) = P_2^{-1}Y(x_1)$ and $K(x_b) = X(x_b)P_1^{-1}$, respectively. Furthermore, the sub-states x_b of the system satisfies the constraint given by (16).

Remark 4: On the basis of Corollary 1, let $\rho = \gamma^2$, the corresponding optimal H_∞ control problem can be converted into the following SOS convex optimisation problem:

$$\begin{aligned}
&\min \quad \rho\\
&\mathrm{s.t.} \quad \begin{cases}(22) - (25)\\ \rho - \varepsilon_0 \in \Phi_{\mathrm{SOS}}\end{cases}
\end{aligned} \tag{26}$$

where ε_0 is a given positive scalar to ensure the positive definiteness of ρ. Then, an optimal H_∞ controller is obtained with the form of (6) and (7), and $\gamma_{\mathrm{opt}} = \sqrt{\rho_{\min}}$.

Remark 5: If $A(x_b)$ in (3), and $X(x_b)$ and $Y(x_1)$ in Corollary 1 also reduce to constant matrices, on the basis of Lemmas 1 and 2, the SOS conditions in (22)–(25) can naturally reduce to the LMI conditions for the Luenberger-OB linear HC problem which has been widely studied in linear control systems [30]. Therefore, Corollary 1 can be treated as an extension of the classical linear HC theory to a non-linear polynomial system.

4 Simulations

The proposed approach of this paper is applied to the flexible spacecraft attitude system in [26]. Considering only the first two modes of the flexible appendages ($N = 2$), the related system parameters are as follows:

$$\begin{aligned}
I_{\mathrm{s}} &= \begin{bmatrix}350 & 3 & 4\\ 3 & 280 & 10\\ 4 & 10 & 190\end{bmatrix}, \quad F_{\mathrm{s}} = \begin{bmatrix}6.45637 & -1.25619\\ 1.27814 & 0.91756\\ 2.15629 & -1.67264\end{bmatrix},\\
\xi &= \begin{bmatrix}0.005607 & 0\\ 0 & 0.00862\end{bmatrix}, \quad \Omega = \begin{bmatrix}0.7681 & 0\\ 0 & 1.1038\end{bmatrix}
\end{aligned}$$

To show the effectiveness and advantages of the proposed non-linear approach, the simulations are performed in the following two parts.

Simulation 1: OBNHC with a given H_∞ performance index

In this case, the H_∞ performance index is given by $\gamma = 0.1$. For computational simplicity, both $X(x_b)$ and $Y(x_1)$ are chosen as polynomial matrices with degree 2, and μ_{1i}, μ_{2j} ($i = 1, 2, 3$, $j = 1, 2, \ldots, 6$) are chosen as positive constants. Moreover, the other simulation parameters are chosen as $\varepsilon_i = 10^{-5}$ ($i = 1, 2, 3, 4$), $\delta_i = 3$ and $\pi_i = 1$ ($i = 1, 2, 3$). By using Corollary 1, an OBNH controller is obtained [Section 8.1.1 of the Appendix].

Furthermore, in order to show the advantages of the proposed approach, an observer-based linear H_∞ controller which is designed by approximately linearising the system in (3)–(5) is chosen as a comparison. In the same simulation environment, an OB linear H_∞ controller is obtained [Section 8.1.2 of the Appendix].

© The Institution of Engineering and Technology 2017

17518652, 2017, 15, Downloaded from https://ietresearch.onlinelibrary.wiley.com/doi/10.1049/iet-cta.2017.0129 by Turkey Cochrane Evidence Aid, Wiley Online Library on [13/09/2023]. See the Terms and Conditions (https://onlinelibrary.wiley.com/terms-and-conditions) on Wiley Online Library for rules of use; OA articles are governed by the applicable Creative Commons License

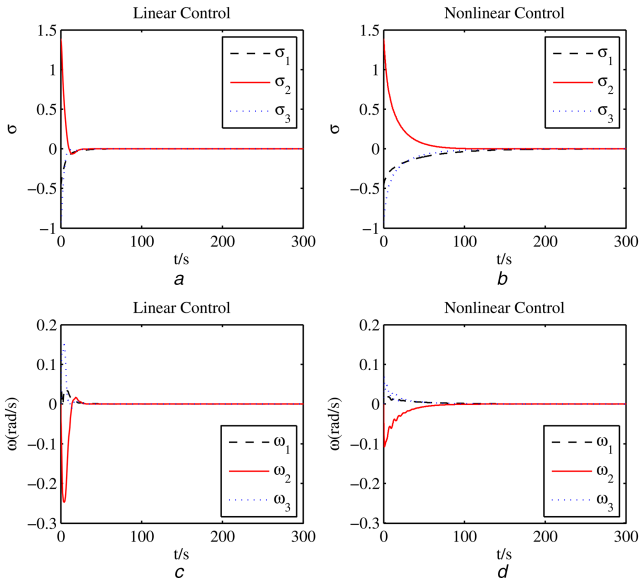


Fig. 1 *Trajectories of σ and ω for the linear control and the proposed non-linear control methods*
(a), (b) Trajectories of σ, ***(c), (d)*** Trajectories of ω

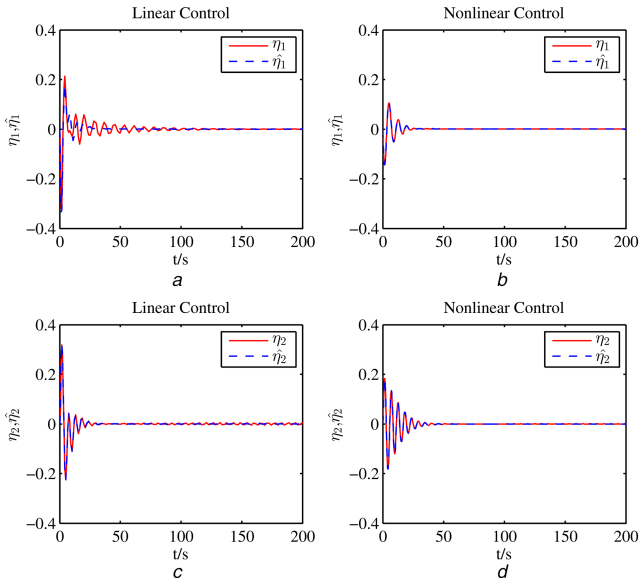


Fig. 2 *Trajectories of η_1, $\hat{\eta}_1$ and η_2, $\hat{\eta}_2$ for the linear control and the proposed non-linear control methods*
(a), (b) Trajectories of η_1, $\hat{\eta}_1$, ***(c), (d)*** Trajectories of η_2, $\hat{\eta}_2$

Suppose the flexible satellite is required to finish the large-angle attitude manoeuvring with the Euler rotation angle $\Theta = 120^{\circ}$ and the Euler principle axis $l = [0.2673 \quad -0.8018 \quad 0.5354]^{\mathrm{T}}$, i.e. the corresponding initial Rodrigues parameters vector is $\sigma(0) = [-0.4630 \quad 1.3888 \quad -0.9258]^{\mathrm{T}}$; the amplitude of the control torque is limited to be no more than 30 N m; the external disturbance and the other initial conditions are chosen as

$$w = \begin{cases} \begin{bmatrix} 0.01 \times \cos(0.05t) \\ 0.02 \\ -0.001 \sin(0.01t) \end{bmatrix}, & 0 < t \le 100 \\ 0, & t > 100 \end{cases}, \quad \omega(0) = \mathbf{0},$$

$$\eta(0) = \varphi(0) = \mathbf{0}, \quad \hat{\eta}(0) = (0) = \hat{\varphi}(0) = \begin{bmatrix} 0.001 \\ -0.001 \end{bmatrix}.$$

The corresponding simulation results of the proposed non-linear control method and the linear control method are shown in Figs. 1–3. Furthermore, to demonstrate the estimation accuracy of the state observer in a quantitative way, the root mean square errors (RMSEs) between the actual values and the estimated values of the flexible modes are computed and shown in Table 1.

As can be seen from Fig. 1, in the same disturbance and the same amplitude limitation of the control input, both the proposed non-linear control method and the linear control method can reach the expected objective with a better convergence property. However, from Fig. 2 and Table 1, we conclude that the non-linear observer can achieve higher state estimation accuracy with less overshoot. Furthermore, in Fig. 3*c*, we apply the proposed non-linear controller and the linear controller to the system in (3)–(5) and specify the disturbance input w as given above with zero initial condition, and then compute the truncated norms $\| z(t) \|_{2,T_0} / \| w(t) \|_{2,T_0}$ to show the actual disturbance attenuation level from the disturbance input w to the controlled output z over finite time interval $[0, T_0]$ with $T_0 = 100$. From Fig. 3*c*, we conclude that the truncated norms for the non-linear control design is less than the one for the linear control design, which indicates a better disturbance attenuation level. Moreover, as expected, the truncated norms are indeed less than $\gamma = 0.1$. Consequently, the proposed non-linear controller can suppress external disturbance with a better level in the process of fast large-angle attitude manoeuvring.

Simulation 2: Observer-based non-linear optimal H_∞ control
In this section, we will search for an optimal value of H_∞ performance index. For computational simplicity, both $X(x_b)$ and $Y(x_1)$ are also chosen as polynomial matrices with degree 2, and μ_{1i}, μ_{2j} ($i = 1, 2, 3$, $j = 1, 2, \ldots, 6$) are chosen as positive constants. Moreover, the other simulation parameters are chosen as $\varepsilon_0 = \varepsilon_1 = \varepsilon_4 = 10^{-6}$, $\varepsilon_2 = 10^{-8}$, $\varepsilon_3 = 10^{-5}$, $\delta_i = 2$ and $\pi_i = 1$ ($i = 1, 2, 3$). By solving the SOS convex optimisation problem formulated in Remark 4, an observer-based non-linear optimal H_∞ controller is obtained with $\gamma_{\mathrm{opt}} = 0.0030$ [Section 8.2.1 of the Appendix]. For comparison, an observer-based linear optimal H_∞ controller is also designed by approximately linearising the system in (3)–(5), and the optimal value of H_∞ performance index for the corresponding closed-loop linear system returns $\gamma_{\mathrm{opt}} = 0.0023$ [Section 8.2.2 of the Appendix].

In this situation, we suppose the flexible satellite is required to finish the attitude manoeuvring with Euler rotation angle $\Theta = 30^{\circ}$ and the Euler principle axis $l = [0.4082 \quad -0.3333 \quad 0.8498]^{\mathrm{T}}$, i.e. the corresponding initial Rodrigues parameters vector is $\sigma(0) = \begin{bmatrix} 0.1094 \\ -0.0893 \\ 0.2277 \end{bmatrix}^{\mathrm{T}}$.

Moreover, the other initial conditions and the external disturbance are chosen as

$$\omega(0) = \mathbf{0}, \ \eta(0) = \mathbf{0}, \ \varphi(0) = \mathbf{0}, \ \hat{\eta}(0) = \hat{\varphi}(0) = \begin{bmatrix} -0.001 \\ 0.001 \end{bmatrix},$$

$$w = \begin{cases} \begin{bmatrix} 0.01 \times \sin(0.05t) \\ 0.05 \\ -0.02 \cos(0.01t) \end{bmatrix}, & 0 < t \le 100 \\ 0, & t > 100 \end{cases}$$

The corresponding simulation results of the proposed non-linear control method and the linear control method are shown in Figs. 4–6. Moreover, the RMSEs between the actual values and the estimated values of flexible modes are also shown in Table 2.

As can be seen from the figures above, both the proposed non-linear control method and the linear control method can reach the expected objective. In Figs. 4 and 6, we observer that though the linear controller achieves a better convergence property in the control of Rodrigues parameters and angular velocity, it requires larger amplitude of control torque. From Figs. 5 and 6 and Table 2, we can conclude that the non-linear controller can achieve a better state estimation accuracy with less overshoot and smaller control torque. Furthermore, for the disturbance input w given above and

© The Institution of Engineering and Technology 2017

17518652, 2017, 15, Downloaded from https://ietresearch.onlinelibrary.wiley.com/doi/10.1049/iet-cta.2017.0129 by Turkey Cochrane Evidence Aid, Wiley Online Library on [13/09/2023]. See the Terms and Conditions (https://onlinelibrary.wiley.com/terms-and-conditions) on Wiley Online Library for rules of use; OA articles are governed by the applicable Creative Commons License

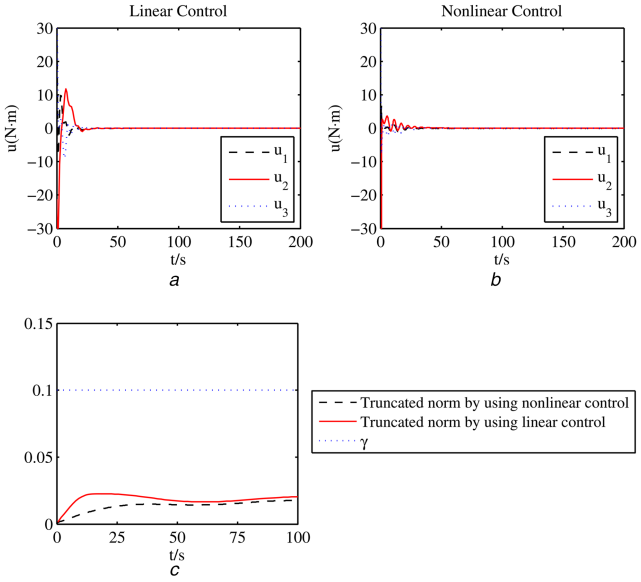


Fig. 3 *Trajectories of u and truncated norms for the linear control and the proposed non-linear control methods*

(a), (b) Trajectories of *u*, ***(c)*** Closed-loop disturbance attenuation for a disturbance input by using the linear control and the proposed non-linear control methods

Table 1 RMSE in Figs. 2*a–d*

Variables of flexible modes	RMSE using linear control	RMSE using non-linear control
η_1, $\hat{\eta}_1$	0.0136	0.0003
η_2, $\hat{\eta}_2$	0.0030	0.0003

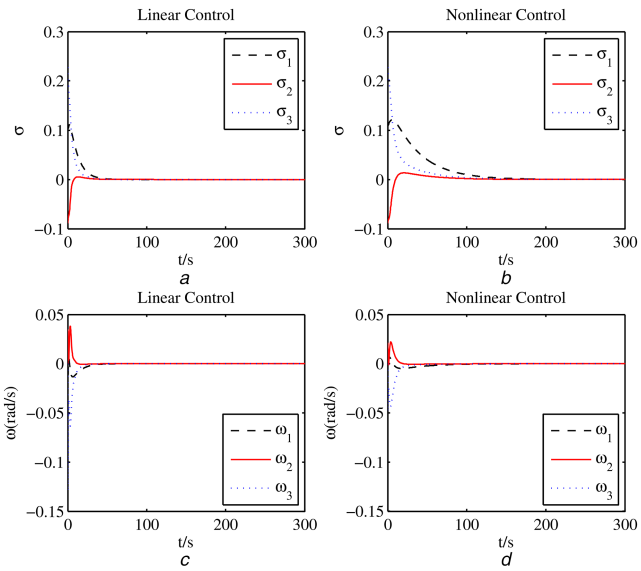


Fig. 4 *Trajectories of σ and ω for the linear control and the proposed non-linear control methods*

(a), (b) Trajectories of *σ*, ***(c), (d)*** Trajectories of *ω*

Table 2 RMSE in Figs. 5*a–d*

Variables of flexible modes	RMSE using linear control	RMSE using non-linear control
η_1, $\hat{\eta}_1$	0.0004	0.0002
η_2, $\hat{\eta}_2$	0.0002	0.0002

zero initial condition, from Fig. 6*c*, we can see that the truncated norms $\| z(t) \|_{2,T_0} / \| w(t) \|_{2,T_0}$ for the non-linear control design is less than the one for the linear control design, which also indicates a better disturbance attenuation performance.

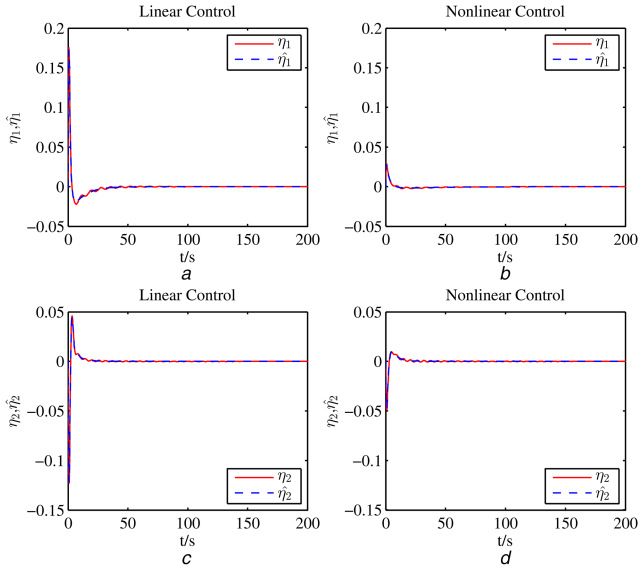


Fig. 5 *Trajectories of η_1, $\hat{\eta}_1$ and η_2, $\hat{\eta}_2$ for the linear control and the proposed non-linear control methods*

(a), (b) Trajectories of η_1, $\hat{\eta}_1$, ***(c), (d)*** Trajectories of η_2, $\hat{\eta}_2$

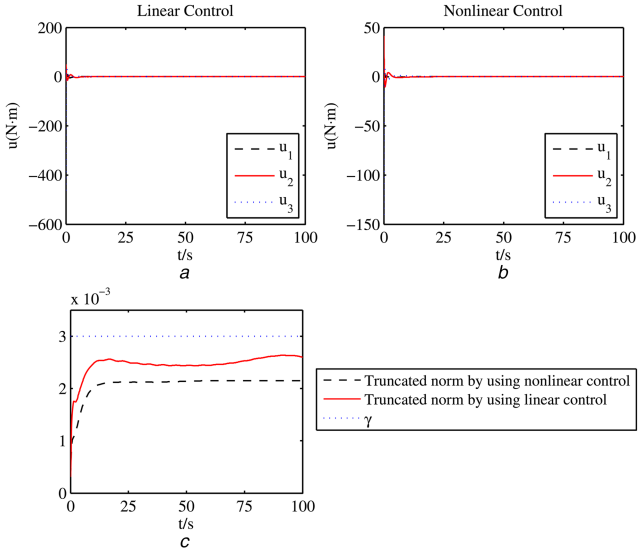


Fig. 6 *Trajectories of u and truncated norms for the linear control and the proposed non-linear control methods*

(a), (b) Trajectories of *u*, ***(c)*** Closed-loop disturbance attenuation for a disturbance input by using the linear control and the proposed non-linear methods

Finally, the computational cost of the simulations is discussed. All simulations are performed on an ordinary Core i7 central processing unit with base frequency of 3.4 GHz. The version of MATLAB is R2013a with SOSTOOLS 3.0. Most of the computational time is spent on solving the feasibility problem formulated in (22)–(25) and the optimisation problem formulated in (26) by SOSTOOLS. For example, the optimisation problem in the second simulation, the most complex case, requires about 3 h to obtain the solutions by SOSTOOLS. For a high-dimensional non-linear polynomial system such as the flexible satellite attitude system considered in this paper, the time-consuming computation is an unavoidable difficulty under the current ordinary processer with the current version of SOSTOOLS.

5 Conclusions

This paper investigates the OBNH attitude control problem for a flexible satellite with external disturbances and state-region constraints. By considering the structural features of the attitude system and using SOS and the generalised *S*-procedure techniques, a convex approach is proposed for the OBNH attitude control

17518652, 2017, 15, Downloaded from https://ietresearch.onlinelibrary.wiley.com/doi/10.1049/iet-cta.2017.0129 by Turkey Cochrane Evidence Aid, Wiley Online Library on [13/09/2023]. See the Terms and Conditions (https://onlinelibrary.wiley.com/terms-and-conditions) on Wiley Online Library for rules of use; OA articles are governed by the applicable Creative Commons License

problem. This approach shows that the above problem can be formulated as an SOS convex optimisation problem, while the reduced-order observer and the non-linear state-feedback controller can be designed independently, thus dramatically reducing the computational complexity and difficulties. Moreover, with the application of a convex optimisation algorithm, the observer and the controller can be analytically constructed and easily implemented in engineering, since they are only the polynomial or rational functions of a system's states. As compared to the classical linear control method in the simulations, the proposed non-linear control method can suppress the external disturbances and flexible vibrations with a better level in the process of attitude manoeuvring. Furthermore, input constraint, uncertainties etc. are also very interesting problems, on this topic, we will adopt the promising intelligent control methods such as adaptive, fuzzy and neural networks based control methods, to address those input non-linearity in the follow-up study.

6 Acknowledgments

The authors would thank the National Natural Science Foundation of China (grant numbers 61374037 and 61673325) for supporting this research.

7 References

[1] Dong, C.Y., Xu, L.J., Chen, Y., *et al.*: 'Networked flexible spacecraft attitude maneuver based on adaptive fuzzy sliding mode control', *Acta Astronaut.*, 2009, **65**, (11-12), pp. 1561–1570

[2] Yang, C.D., Sun, Y.P.: 'Mixed H_2/H_∞ state-feedback design for micro-satellite attitude control', *Control Eng. Pract.*, 2002, **10**, (9), pp. 951–970

[3] Wang, H.Q, Liu, X.P., Liu, K.F.: 'Adaptive fuzzy tracking control for a class of pure-feedback stochastic nonlinear systems with non-lower triangular structure', *Fuzzy Sets Syst.*, 2016, **302**, (1), pp. 101–120

[4] Chen, B., Lin, C., Liu, X.P., *et al.*: 'Observer-based adaptive fuzzy control for a class of nonlinear delayed systems', *IEEE Trans. Syst. Man Cybern. Syst.*, 2016, **46**, (1), pp. 27–36

[5] Sun, H.F., Yang, Z.L., Meng, B.: 'Tracking control of a class of non-linear systems with applications of cruise control of hypersonic vehicles', *Int. J. Control*, 2015, **88**, (5), pp. 885–896

[6] Wang, H.Q., Liu, K.F., Liu, X.P., *et al.*: 'Neural-based adaptive output-feedback control for a class of nonstrict-feedback stochastic nonlinear systems', *IEEE Trans. Cybern.*, 2015, **45**, (9), pp. 1977–1987

[7] Fazlyab, A.R., Saberi, F.F., Kabganian, M.: 'Adaptive attitude controller for a satellite based on neural network in the presence of unknown external disturbances and actuator faults', *Adv. Space Res.*, 2016, **57**, (1), pp. 367–377

[8] Wu, S.N., Wen, S.H.: 'Robust H_∞ output feedback control for attitude stabilization of a flexible spacecraft', *Nonlinear Dyn.*, 2016, **84**, (1), pp. 405–412

[9] Sun, H.F., Yang, Z.L., Zeng, J.P.: 'New tracking-control strategy for airbreathing hypersonic vehicles', *J. Guid. Control Dyn.*, 2013, **36**, (3), pp. 846–859

[10] Prempain, E.: 'An application of the sum of squares decomposition to the L_2 gain computation for a class of nonlinear systems'. Proc. 44th IEEE Conf. Decision and Control, Seville, Spain, December 2005, pp. 6865–6868

[11] Krug, M., Staa, A., Nguang, S.: 'Robust H_∞ static output feedback controller design for parameter dependent polynomial systems: an iterative sum of squares approach', *J. Franklin Inst.*, 2013, **350**, (2), pp. 318–330

[12] Prajna, S., Papachristodoulou, A., Wu, F.: 'Nonlinear control synthesis by sum of squares optimization: a Lyapunov-based approach'. Proc. Fifth Asian Control Conf., Melbourne, Australia, July 2004, pp. 157–165

[13] Nguang, S.K., Saat, S., Krug, M.: 'Static output feedback controller design for uncertain polynomial systems: an iterative sum of squares approach', *IET Control Theory Appl.*, 2011, **5**, (9), pp. 1079–1084

[14] Gollu, N., Rodrigues, L.: 'Control of large angle attitude maneuvers for rigid bodies using sum of squares'. Proc. American Control Conf., New York, USA, 2007, pp. 3156–3161

[15] Gollu, N.: 'Switched control of satellites for global stabilization and local performance: a sum of squares approach'. Proc. American Control Conf., Washington, DC, USA, 2008, pp. 2987–2992

[16] Zheng, M., Wang, J: 'Applying back-stepping and LPV control strategy to improve satellite attitude maneuver performance', *Electr. Mach. Control*, 2010, **14**, (9), pp. 100–106

[17] Capua, A., Shapiro, A., Choukroun, D.: 'Robust nonlinear H_∞ output-feedback for spacecraft attitude control'. AIAA Guidance, Navigation, and Control Conf., National Harbor, MD, January 2014

[18] Zheng, Q., Wu, F.: 'Generalized nonlinear H_∞ synthesis condition with its numerically efficient solution', *Int. J. Robust Nonlinear Control*, 2011, **21**, (18), pp. 2079–2100

[19] Zhou, Y.R., Zeng, J.P.: 'Observer-based robust stabilization for a class of uncertain polynomial systems', *Trans. Inst. Meas. Control*, 2017, **39**, (5), pp. 675–687

[20] 'Sostools: sum of squares optimization toolbox for MATLAB: user's guide version 3.0'. Available at http://www.cds.caltech.edu/sostools/, accessed 16 October 2013

[21] Parrilo, P.A.: 'Semidefinite programming relaxations for semialgebraic problems', *Math. Program. B*, 2003, **96**, (2), pp. 293–320

[22] Jarvis-Wloszek, Z.W.: 'Lyapunov based analysis and controller synthesis for polynomial system using sum-of-squares optimization'. PhD thesis, University of California, 2003

[23] Shuster, M.D.: 'A survey of attitude representations', *J. Astronaut. Sci.*, 1993, **41**, (4), pp. 439–517

[24] Sidi, M.J.: '*Spacecraft dynamics and control: a practical engineering approach*' (Cambridge University Press, UK, 1997)

[25] Gennaro S., Di: 'Active vibration suppression in flexible spacecraft attitude tracking', *J. Guid. Control Dyn.*, 1998, **21**, pp. 400–408

[26] Gennaro S., Di: 'Output stabilization of flexible spacecraft with active vibration suppression', *IEEE Trans. Aerosp. Electron. Syst.*, 2003, **39**, (3), pp. 747–759

[27] Hu, Q.L.: 'Robust adaptive back-stepping attitude and vibration control with L_2-gain performance for flexible spacecraft under angular velocity constraint', *J. Sound Vibr.*, 2009, **327**, pp. 285–298

[28] Zheng, D.Z.: '*Linear system theory*' (Tsinghua University Press, Beijing, 2002)

[29] Lin, C., Wang, Q.G., Lee, T.H., *et al.*: 'Observer-based H_∞ fuzzy control design for T–S fuzzy systems with state delays', *Automatica*, 2008, **44**, (3), pp. 868–874

[30] Boyd, S., El Ghaoui, L., Feron, E., *et al.*: '*Linear matrix inequalities in system and control theory*' (Society for Industrial and Applied Mathematics, Philadelphia, 1994)

8 Appendix

For the sake of simplicity in formula, we first define

$$\chi_\sigma = \left[1,\ \sigma_1,\ \sigma_2,\ \sigma_3,\ \sigma_1^2,\ \sigma_1\sigma_2,\ \sigma_1\sigma_3,\ \sigma_2^2,\ \sigma_2\sigma_3,\ \sigma_3^2\right]^{\mathrm{T}}$$

$$\begin{aligned}\chi_{\sigma,\omega} = \big[&1,\ \sigma_1,\ \sigma_2,\ \sigma_3,\ \omega_1,\ \omega_2,\ \omega_3,\ \sigma_1^2,\ \sigma_1\sigma_2,\ \sigma_1\sigma_3,\\ &\sigma_1\omega_1,\ \sigma_1\omega_2,\ \sigma_1\omega_3,\ \sigma_2^2,\ \sigma_2\sigma_3,\ \sigma_2\omega_1,\ \sigma_2\omega_2,\\ &\sigma_2\omega_3,\ \sigma_3^2,\ \sigma_3\omega_1,\ \sigma_3\omega_2,\ \sigma_3\omega_3,\ \omega_1^2,\ \omega_1\omega_2,\\ &\omega_1\omega_3,\ \omega_2^2,\ \omega_2\omega_3,\ \omega_3^2\big]^{\mathrm{T}}\end{aligned}$$

8.1 Appendix 1. The non-linear and linear controllers used in simulation 1

8.1.1 Non-linear controller used in Simulation 1: Owing to the space limitation, only the first row of the non-linear observer gain matrix $L(x_1) = \left(l_{ij}(x_1)\right)_{4\times 6}$ and the first column of non-linear controller gain matrix $K(x_b) = \left(k_{ij}(x_b)\right)_{3\times 10}$ are given herein

$$l_{11}(x_1) = l_{12}(x_1) = l_{13}(x_1) = 0$$

$$\begin{aligned}l_{14}(x_1) = \big[&3.8496,\ 3.9986\times 10^{-9},\ -1.8883\times 10^{-9},\\ &-2.0599\times 10^{-10},\ 3.0054,\ 1.6697\times 10^{-9},\\ &4.5254\times 10^{-9},\ 3.0058,\ 2.7397\times 10^{-9},\\ &3.0058\big]\chi_\sigma\end{aligned}$$

$$\begin{aligned}l_{15}(x_1) = \big[&0.7642,\ 3.3710\times 10^{-10},\ 1.0238\times 10^{-9},\\ &4.0449\times 10^{-9},\ 1.2893,\ 9.8192\times 10^{-10},\\ &4.4206\times 10^{-9},\ 1.2894,\ -1.8235\times 10^{-10},\\ &1.2895\big]\chi_\sigma\end{aligned}$$

$$\begin{aligned}l_{16}(x_1) = [&2.2441,\ 3.0391\times 10^{-9},\ -3.2704\times 10^{-9},\\ &-6.4586\times 10^{-9},\ 0.6771,\ -3.5834\times 10^{-11},\\ &-2.8267\times 10^{-9},\ 0.6774,\ 2.7235\times 10^{-9},\\ &0.6773]\chi_\sigma\end{aligned}$$

© The Institution of Engineering and Technology 2017

17518652, 2017, 15, Downloaded from https://ietresearch.onlinelibrary.wiley.com/doi/10.1049/iet-cta.2017.0129 by Turkey Cochrane Evidence Aid, Wiley Online Library on [13/09/2023]. See the Terms and Conditions (https://onlinelibrary.wiley.com/terms-and-conditions) on Wiley Online Library for rules of use; OA articles are governed by the applicable Creative Commons License

$$\zeta_{11}(x_b) = [-126.0464,\ -0.4264,\ 18.6739,\ -9.6183,\ -0.1456\ -5.4800,\ 3.5109,\ -113.9557,\ 6.8722,\ 13.6266,\ -0.0741,\ 0.1199,\ 0.1034,\ -100.3064,\ 1.0385,\ -0.0278,\ 0.1834,\ 0.0288,\ -99.7188,\ -0.0570,\ 0.0552,\ 0.1662,\ -100.7342,\ 0.3279,\ 0.7314,\ -102.6866,\ 0.4364,\ -102.7675]\chi_{\sigma,\omega}$$

$$k_{21}(x_b) = [-12.1662,\ -2.0019,\ -9.2457,\ 42.7581,\ 4.4254,\ 1.9884,\ -22.3642,\ -8.7384,\ -35.0965,\ -6.6252,\ 0.1137,\ -0.4055,\ -0.1788,\ -17.5375,\ -2.3827,\ -0.0769,\ -0.0447,\ 0.0289,\ -16.5935,\ 0.0222,\ -0.1289,\ 0.0107,\ -16.3927,\ 1.3671,\ 0.1023,\ -16.1399,\ 0.4761,\ -16.4117]\chi_{\sigma,\omega}$$

$$\zeta_{31}(x_b) = [-20.7215,\ 1.5025,\ -39.0214,\ 6.8797,\ -2.0299,\ 21.5009,\ -2.7779,\ -15.0825,\ -5.1034,\ -34.0567\ 0.2846,\ 0.0392,\ -0.4966,\ -24.8786,\ -1.7891,\ 0.0305,\ -0.0715,\ -0.0729,\ -25.6037,\ -0.1205,\ -0.0214,\ -0.0899,\ -25.4584,\ 0.2241,\ 2.8985,\ -25.6959,\ 0.2833,\ -25.0248]\chi_{\sigma,\omega}$$

8.1.2 Linear controller used in Simulation 1: The linear observer gain matrix L and the linear controller gain matrix K are given herein

$$L = \begin{bmatrix} 0 & 0 & 0 & 2.8705 & 0.5713 & 1.6835 \\ 0 & 0 & 0 & -0.5636 & 0.4732 & -1.2439 \\ 0 & 0 & 0 & 0.0572 & 0.0401 & -0.0251 \\ 0 & 0 & 0 & -0.1837 & -0.0266 & -0.0846 \end{bmatrix}$$

$$K = \begin{bmatrix} -63.9394 & -1.5127 & -10.0086 & -463.6939 \\ -14.9889 & -43.1260 & -34.2309 & -189.8667 \\ -3.1304 & 4.5095 & -36.2929 & -89.6522 \\ -75.9442 & -111.4167 & 55.3933 & -16.3658 \\ -156.6535 & -122.0661 & 30.8338 & -5.7875 \\ 23.8146 & -143.2743 & 7.6277 & -31.7745 \\ 7.7261 & 16.7952 \\ 4.3868 & 13.8849 \\ 0.5316 & -14.2002 \end{bmatrix}$$

8.2 Appendix 2: The non-linear and linear controllers used in Simulation 2

8.2.1 Non-linear controller used in Simulation 2: Owing to the space limitation, only the first row of the non-linear observer gain matrix $L(x_1) = \left(l_{ij}(x_1)\right)_{4\times 6}$ and the first column of non-linear the controller gain matrix $K(x_b) = \left(k_{ij}(x_b)\right)_{3\times 10}$ are given herein

$$l_{11}(x_1) = l_{12}(x_1) = l_{13}(x_1) = 0$$

$$l_{14}(x_1) = [3.8252,\ 3.0753\times 10^{-10},\ 2.0281\times 10^{-11},\ 1.4816\times 10^{-10},\ 2.9815,\ -4.6184\times 10^{-10},\ 5.2627\times 10^{-10},\ 2.9815,\ -8.8785\times 10^{-10},\ 2.9815]\chi_{\sigma}$$

$$l_{15}(x_1) = [0.8239,\ 2.7739\times 10^{-10},\ -1.1716\times 10^{-10},\ -8.0799\times 10^{-11},\ 1.3239,\ 9.8167\times 10^{-11},\ 9.3312\times 10^{-11},\ 1.3239,\ -1.2201\times 10^{-11},\ 1.3239]\chi_{\sigma}$$

$$l_{16}(x_1) = [2.2641,\ -1.4681\times 10^{-10},\ 2.0126\times 10^{-10},\ 2.6322\times 10^{-10},\ 0.7029,\ -5.8112\times 10^{-10},\ 3.4268\times 10^{-10},\ 0.7029,\ -8.0428\times 10^{-10},\ 0.7029]\chi_{\sigma}$$

$$k_{11}(x_b) = [-654.1895,\ -0.2674,\ 263.5256,\ -131.3429,\ -0.2602,\ -14.72519,\ 9.1763,\ -451.1144,\ 100.8984,\ 205.4720,\ -0.0313,\ -0.0070,\ 0.5942,\ -211.9454,\ 21.3189,\ -0.0285,\ 0.2219,\ 0.0620,\ -196.1887,\ -0.0714,\ 0.0431,\ 0.2855,\ -271.5826,\ 0.4359,\ 1.0097,\ -220.0924,\ -0.5496,\ -220.0964]\chi_{\sigma,\omega}$$

$$\zeta_{21}(x_b) = [7.3153,\ -53.1122,\ -104.8516,\ 609.2126,\ 11.8126,\ 4.7682,\ -55.7013,\ 67.8387,\ -573.4342,\ -77.8626\ 0.1993,\ -0.4116,\ -0.0025,\ -60.0667,\ -57.9650,\ -0.0934,\ -0.0282,\ 0.0012,\ -40.4420,\ 0.0397,\ -0.1591,\ 0.0205,\ -32.7081,\ 1.7981,\ 0.1567,\ -32.3603,\ 0.5995,\ -32.6781]\chi_{\sigma,\omega}$$

$$\zeta_{31}(x_b) = [-112.7302,\ 19.3352,\ -541.5822,\ 74.2910,\ -4.9720\ 51.5619,\ -6.5061,\ 76.4018,\ -56.5715,\ -499.8754,\ -0.2629,\ 0.0118,\ -0.5674,\ -55.9474,\ -30.4296,\ 0.0092,\ -0.0440,\ -0.0924,\ -100.4070,\ -0.2108,\ -0.0061,\ -0.1403,\ -54.3271,\ 0.4074,\ 3.8695,\ -54.5822,\ 0.2790,\ -53.4513]\chi_{\sigma,\omega}$$

8.2.2 Linear controller used in Simulation 2: The linear observer gain matrix L and the linear controller gain matrix K are given herein

$$L = \begin{bmatrix} 0 & 0 & 0 & 2.8552 & 0.6134 & 1.6993 \\ 0 & 0 & 0 & -0.5623 & 0.4632 & -1.2427 \\ 0 & 0 & 0 & 0.0572 & 0.0408 & -0.0168 \\ 0 & 0 & 0 & -0.1828 & -0.0290 & -0.1171 \end{bmatrix}$$

$$K = \begin{bmatrix} -1.8772 & -0.0740 & -0.3299 & -3.5175 \\ -0.3293 & -1.3232 & -0.4605 & -0.7180 \\ -0.2978 & 0.2922 & -1.7732 & -1.0316 \\ -0.4099 & -0.7530 & 1.0599 & -0.0842 \\ -1.8226 & -0.4899 & 0.4661 & 0.6394 \\ 0.3773 & -2.5668 & 0.2531 & -1.3681 \\ -0.9813 & 0.1884 \\ -0.4346 & -0.1789 \\ -0.2486 & 0.7464 \end{bmatrix} \times 10^3$$

© The Institution of Engineering and Technology 2017

17518652, 2017, 15, Downloaded from https://ietresearch.onlinelibrary.wiley.com/doi/10.1049/iet-cta.2017.0129 by Turkey Cochrane Evidence Aid, Wiley Online Library on [13/09/2023]. See the Terms and Conditions (https://onlinelibrary.wiley.com/terms-and-conditions) on Wiley Online Library for rules of use; OA articles are governed by the applicable Creative Commons License